Figure 4. SF-RS spectra for the $ClO_2^--Cu^{2+}$ system. Each spectrum is the average of the first three to five consecutive scans. Scan rate: 190 nm/100 ms. Dashed line: 0.500 M $NaClO_2$. Dotted line: 0.157 M $Cu(ClO_4)_2$. Solid lines: $C_{ClO_2^-} = 5.01 \times 10^{-3}$ M and $C_{Cu^{2+}} = 6.97 \times 10^{-3}$, 1.39×10^{-2}, 3.49×10^{-2}, 6.97×10^{-2}, 0.105, and 0.157 M in the order of increasing absorbance. $C_{H^+} = 7.0 \times 10^{-4}-1.1 \times 10^{-3}$ M.

experiments clearly prove the formation of a new species.

The data, evaluated by using Job's method[22] (Figure 3), are consistent with the formation of a complex with 1:1 stoichiometry for ClO_2^- and Cu^{2+} (reaction 2). The evaluation of the data based on the Coleman–Varga method[23] led to the same conclusion.

$$Cu^{2+} + ClO_2^- = CuClO_2^+ \qquad (2)$$

At higher reactant concentrations, and at longer times, the spectra seemingly were somewhat corrupted by the formation of ClO_2. Considering the applied experimental conditions (pH = 2.5–3.5), this observation indicates that Cu^{2+} slightly catalyzes the decomposition of chlorite ion.

The SF-RS measurements were performed by varying the Cu^{2+} and ClO_2^- concentrations in the range of $1.39 \times 10^{-3}-0.157$ and $1.00 \times 10^{-3}-0.500$ M, respectively. The acid concentration of these samples was $5 \times 10^{-4}-1.0 \times 10^{-3}$ M. In general, the rate of the complex formation reactions with Cu^{2+} is close to the diffusion-controlled limit.[24] Accordingly, the formation of the $CuClO_2^+$ complex was completed in less than the dead time of the SF-RS measurements. No apparent change was observed in the consecutive rapid-scan spectra, even when the fastest available scan rate (190 nm/2 ms) was applied. A few representative spectra are shown in Figure 4. A similar concentration dependence was observed with chlorite ion.

The data for 15 wavelengths in the 360–480-nm wavelength range were evaluated with the program PSEQUAD.[25] In these calculations, the pK_a of $HClO_2$ and the spectrum of the chlorite ion were included as known parameters, and the stability constant as well as the spectrum of the $CuClO_2^+$ complex were simultaneously evaluated. The Job's curves calculated with the fitted parameters are in excellent agreement with the experimental data from standard spectrophotometric measurements (Figure 3).

The calculated stability constant for the $CuClO_2^+$ complex is 1.04 ± 0.07 M^{-1}. The molar absorptivity of this species at the maximum wavelength, 387 nm, is 1990 ± 120 M^{-1} cm^{-1}. As expected, a relatively weak complex is formed with Cu^{2+}, although its stability is considerably higher than that of the uranyl complex.[9] The complex formation is associated with the appearance of an intense, presumably charge-transfer, band in the near-UV–visible spectral region. The main implication of these results is that the complex formation can be part of any reaction system including a transition-metal ion and ClO_2^-. Most likely, these complexes

are rapidly formed at even relatively low concentration levels. However, they may be of crucial kinetic importance in the oxidation–reduction and catalytic decomposition reactions of chlorite ion. The results also indicate that proper characterization of these complexes requires the application of fast spectrophotometric methods. This subject has been addressed in our ongoing equilibrium and kinetic studies.

Contribution from the Department of Chemistry, University of Helsinki, Et. Hesperiankatu 4, 00100 Helsinki, Finland

The Large Range of Uranyl Bond Lengths: Ab Initio Calculations on Simple Uranium–Oxygen Clusters

Pekka Pyykkö* and Yongfang Zhao†

The large range of uranyl bond lengths is a classical problem.[1] We present here an ab initio study of the underlying mechanism, supposing it to be an intramolecular one, taking place inside an axial + equatorial, $[(O_{ax}UO_{ax})(O_{eq})_n]^{6-}$ ($n = 4$) distorted octahedral model cluster, including the UO_2^{m+} ($m = 0-2$), "antiuranyl" $UO_4^{2-}(D_{4h})$ and cubic UO_6^{6-} limits.
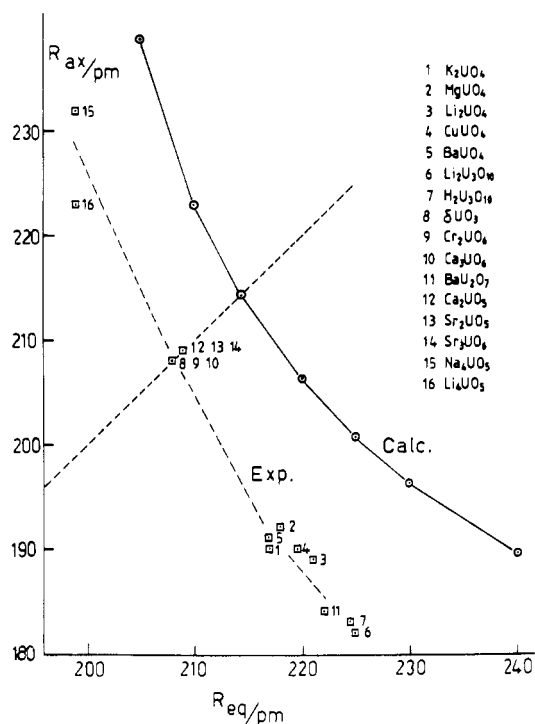
The quasirelativistic pseudopotential of Hay et al.[2] and Gaussian 90[3] were used. The oxygen basis is described in ref 4. For a possible explanation as to why structural calculations on highly charged anions work, see ref 5. The calculated bond lengths and breathing frequencies are given in Table I.

The free UO_2^{m+} bond length and its charge dependence resemble earlier studies and are for uranyl near the low end of the experimental range of about 150–208 pm.[1a] The UO_4^{2-} one is a little below and the UO_6^{6-} one a little above experiment. Taking then U–O$_{eq}$ as the independent variable and optimizing U–O$_{ax}$, we find the results shown in Figure 1. They nicely parallel the

---

†On leave from the Institute of Atomic and Molecular Physics, Jilin University, 130023 Changchun, People's Republic of China.

(1) (a) Denning, R. G. *Gmelin Handbook, U Supplement A6*; Springer: Berlin, 1983; pp 31–79. (b) Katz, J. J.; Seaborg, G. T.; Morss, L. R. *The Chemistry of the Actinide Elements*, 2nd ed.; Chapman and Hall: London and New York, 1986; Vol. 1. (c) Jørgensen, C. K.; Reisfeld, R. *Structure Bonding* **1982**, *50*, 121–171 (see p 155). (d) Glebov, V. A. *Electronic Structure and Properties of Uranyl Compounds* (in Russian); Energoatomizdat: Moscow, 1983.
(2) Hay, P. J.; Wadt, W. R.; Kahn, L. R.; Raffenetti, R. C.; Phillips, D. H. *J. Chem. Phys.* **1979**, *71*, 1767–1779.
(3) Frisch, M. J.; Head-Gordon, M.; Trucks, G. W.; Foresman, J. B.; Schlegel, H. B.; Raghavachari, K.; Robb, M. A.; Binkley, J. S.; Gonzalez, C.; Defrees, D. J.; Fox, D. J.; Whiteside, R. A.; Seeger, R.; Melius, C. F.; Baker, J.; Martin, R. L.; Kahn, L. R.; Stewart, J. J. P.; Topiol, S.; Pople, J. A. *Gaussian 90*; Gaussian, Inc.: Pittsburgh PA, 1990.
(4) Wadt, W. R. *J. Am. Chem. Soc.* **1981**, *103*, 6053.
(5) Pyykkö, P.; Zhao, Y.-F. *J. Phys. Chem.* **1990**, *94*, 7753–7759.
(6) van Wezenbeek, E. M.; Baerends, E. J.; Snijders, J. G. Submitted for publication. This paper contains a good summary of earlier calculations on uranyl.
(7) Green, D. W.; Gabelnick, S. D.; Reedy, G. T. *J. Chem. Phys.* **1976**, *64*, 1697–1705.
(8) Allen, G. C.; Baerends, E. J.; Vernooijs, P.; Dyke, J. M.; Ellis, A. M.; Fehér, M.; Morris, A. *J. Chem. Phys.* **1988**, *89*, 5363–5372.
(9) Gabelnick, S. D.; Reedy, G. T.; Chasanov, M. G. *J. Chem. Phys.* **1973**, *58*, 4468–4475.
(10) Hoekstra, H.; Siegel, S. *J. Inorg. Nucl. Chem.* **1964**, *26*, 693–700.

---

(22) Job, P. *Ann. Chim. Phys.* **1928**, *9*, 113.
(23) Coleman, I. S.; Varga, L. P. *Inorg. Chem.* **1970**, *9*, 1015.
(24) Margerum, D. W.; Cayley, G. R.; Weatherburn, D. C.; Pagenkopf, G. K. In *Coordination Chemistry*; Martell, A. E., Ed.; American Chemical Society: Washington, DC, 1978; Vol. 2, p 1 and references therein.
(25) Zékány, L.; Nagypál, I. In *Computational Methods for the Determination of Formation Constants*; Leggett, D. J., Ed.; Plenum: New York, 1985; p 291.

Figure 1. Optimized R_{ax} as a function of R_{eq} for UO_6^{6-} clusters. The experimental points are taken from refs 1d and 10.
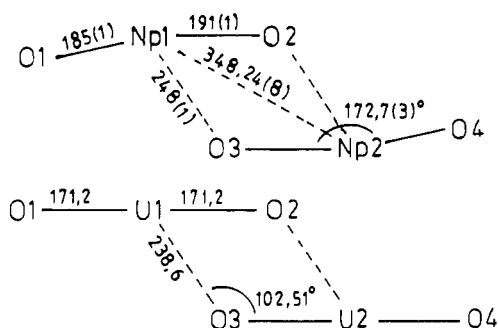
Figure 2. (a) Experimental geometry for $(ONpO^+)_2$ in $Na_4(NpO_2)_2\cdot C_{12}O_{12}\cdot 8H_2O$.[12] (b) Calculated geometry in a $(OUO^+)_2$ model dimer ($S = 1$). Only the dimer parameters O_2-U_2 and $O_2-U_1-O_3$ are optimized.

experimental trend. The intramolecular total energy changes only very little over the range given.[11] Thus we interpret the large

Table I. Calculated Relativistic U–O Bond Lengths, R (in pm), and Breathing Frequencies $\nu_1(a_1)$ (in cm^{-1})

species	method	R	ν_1	ref
UO_2^{2+}	HF	162.5	1216	
	MP2	173.2	922	
	HF	163		a
	HFS	170.0		b
	exptl		ca. 830	c
UO_2^+	HF	171.2	1031	
	MP2	177.0	1074	
	exptl		808	d
UO_2	HF	181.8		e
	MP2	179.7		
	HFS	187.3		f
	HFS	183.4		b
	exptl		765	g
UO_4^{2-}	HF	187.3	872	
	exptl	199		h
UO_6^{6-}	HF	214.8	592	
	exptl	208–209		i
	exptl		797	j
UN_2	HF	181.8	783	
	MP2	191.1	816	

[a] Reference 4. [b] Reference 6. [c] A typical value for U–O_{ax} around 170 pm.[1d] [d] Reference 7 (average). [e] Purposely omitted for this single-configuration open-shell $\phi^1\delta^1$ triplet state. [f] Reference 8. [g] Reference 9. [h] In Na_4UO_5 and Li_4UO_5.[10] [i] See Figure 1. [j] Reference 1c.

range of U–O_{ax} distances as a soft e_g vibrational mode (axial in–equatorial out, or vice versa) of the cubic UO_6^{6-} cluster, which is frozen in by the lattice forces, totally neglected here.

For Np, a peculiar $(ONpO^+)_2$ dimer was found by Cousson et al.[12] (Figure 2a). For a dimer of linear, symmetrical (OUO^+) groups ($R = 171.2$ pm) we indeed find the stable geometry in Figure 2b. Hence also this structure could be explained by intramolecular interactions.

(11) The cubic symmetry is an energy minimum. The force constant $\partial^2 E/\partial R_{eq}^2$ for the minimum-energy path in Figure 1 at $R_{eq} = R_{ax} = 214.4$ pm is only 0.14 au, compared to 1.31 au for the breathing (a_{1g}) mode.
(12) Cousson, A.; Dabos, S.; Abazli, H.; Nectoux, F.; Pagès, M.; Choppin, G. *J. Less-Common Met.* **1984,** *99,* 233.

Additions and Corrections

1990, Volume 29

S. K. Xi, H. Schmidt, C. Lensink, S. Kim, D. Wintergrass, L. M. Daniels, R. A. Jacobson, and J. G. Verkade*: Bridgehead–Bridgehead Communication in Untransannulated $ZP(ECH_2CH_2)_3N$ Systems.

Pages 2215, 2216, and 2219. The oxygens in structure **8** should be replaced by nitrogens, the captions for Figures 1 and 2 should be interchanged, and the nitrogen in structure **16** should be replaced by a phosphorus.—J. G. Verkade